

# A Model for Dark Matter Halos

F.D.A. Hartwick

*Department of Physics and Astronomy,  
University of Victoria, Victoria, BC, Canada, V8W 3P6*

## ABSTRACT

A halo model is presented which possesses a constant phase space density (Q) core followed by a radial CDM-like power law decrease in Q. The motivation for the core is the allowance for a possible primordial phase space density limit such as the Tremaine-Gunn upper bound. The space density profile derived from this model has a constant density core and falls off rapidly beyond. The new model is shown to improve the fits to the observations of LSB galaxy rotation curves, naturally provides a model which has been shown to result in a lengthened dynamical friction time scale for the Fornax dwarf spheroidal galaxy and predicts a flattening of the density profile within the Einstein radius of galaxy clusters. A constant gas entropy floor is predicted whose adiabatic constant provides a lower limit in accord with observed galaxy cluster values. While ‘observable-sized’ cores are not seen in standard cold dark matter (CDM) simulations, phase space considerations suggest that they could appear in warm dark matter (WDM) cosmological simulations and in certain hierarchically consistent SuperWIMP scenarios.

*Subject headings:* cosmology: dark matter

## 1. Introduction

Simulations of cold dark matter (CDM) cosmology predict halos whose density profiles are generally well described by what has become known as an NFW profile (Navarro et al. 1997). A defining characteristic is the presence of a density cusp at the center. Another important property of CDM halo profiles is that they exhibit a power law in the parameter  $\rho/\sigma^3$  which extends over two orders of magnitude in radius beyond the resolution limit of the simulations. This was first shown by Taylor & Navarro (2001) from modelling based on the NFW density profile and later directly from CDM simulations by Dehnen & McLaughlin (2005). Nonparametric models of the density profiles of CDM halos as well as alternate

parameterizations are given by Merritt et al. (2006). In a companion paper Graham et al. (2006) discuss the power law nature of the  $\rho/\sigma^3$  profile.

The NFW profile has been successfully fit to many observations including those of dwarf spheroidal and low surface brightness (LSB) galaxies as well as galaxy clusters. However, not all LSB rotation curves can be fit (Hayashi et al. 2004), and some authors have reported density profiles near the centers of galaxy clusters which are shallower than predicted by NFW (e.g. Sand et al. 2002, Broadhurst et al. 2005). Recently, Goerdt et al. (2006) have argued that a constant density core is required in the Fornax dwarf in order to understand why its resident globular clusters have not disappeared due dynamical friction, as might be expected if its dark matter halo was of NFW form. Modelling dark matter halos with constant density cores is not new but it is usually done by parameterizing the density profile (e.g. see Burkert, 1995 and references above). Here the goal is to follow the effects of a finite primordial phase space density upper limit. Thus the constant density core results from a solution of the Jeans equation with a parameterized phase space density profile.

Simple analytical arguments suggest that the effects of a primordial phase space density bound should be seen in present structures even after many mergings (e.g. Dalcanton & Hogan, 2001). In the absence of cosmological simulations which include such a primordial bound, we rely here on the good agreement of predictions from a simple model with observations to argue that standard CDM simulations and hence the NFW profile may not be giving a complete picture.

## 2. The Model

We start with a CDM like power law in the quantity  $\rho/\sigma^3$  where  $\rho$  is the local space density and  $\sigma$  is the local radial velocity dispersion. The above quantity is often loosely referred to as the phase space density (as it is here) but it is actually a ‘pseudo’ phase space density (e.g. see Dekel & Arad (2004) for a discussion of the true 6-D phase space density). This power law is maintained in the outer regions of the model but with a continued rise at sufficiently small radius, the phase space density is assumed to reach the Tremaine & Gunn (1979) limit in the absence of other lower and less fundamental limiting effects. This quantum statistical upper limit on the phase space density applies to thermal particles as well as fermions. Hence, as long as the particles are not bosons we expect an eventual cap/core in the central phase space density. Here a simple model is proposed in order to mimic the lingering effects of a putative but as yet unknown primordial phase space density bound ( $Q_p \equiv \bar{\rho}/\bar{\sigma}^3$  where  $\bar{\rho}$  is the mean density and  $\bar{\sigma}$  is the one dimensional velocity dispersion). With a constant central phase space density ( $Q_o$ ) core of size  $r_c$ , the following profile is

defined:

$$\rho/\sigma^3 \equiv Q(r) = \frac{Q_o}{(1 + (r/r_c)^\alpha)^{1.92/\alpha}} \quad (1)$$

The choice of a model independent power law index of 1.92 (close to that found by Taylor & Navarro) comes from the work of Dehnen & McLaughlin (2005). All but one of the models presented here were computed with the shape parameter  $\alpha = 1.92$ . Lower values of  $\alpha$  result in a more gradual transition to the outer power law and as will be shown produce very similar results.

The above expression for  $Q(r)$  is substituted into the Jeans equation after eliminating  $\sigma^2$ , thereby allowing the determination of the density profile  $\rho$ . (Note the assumption of spherical symmetry).

$$\frac{d \log \rho}{d \log r} = -0.6 \frac{GM_r}{r} \left( \frac{Q}{\rho} \right)^{2/3} - 1.2\beta + 0.4 \frac{d \log Q}{d \log r} \quad (2)$$

with

$$\frac{dM_r}{d \log r} = \ln(10) 4\pi r^3 \rho \quad (3)$$

where  $\beta$  is the anisotropy parameter (Binney & Tremaine, 1987) and is positive for a predominantly radial anisotropy. The following dimensionless number involving the initial conditions was found to lie between 2 and 3 for all models presented here.

$$\gamma = 4\pi G r_c^2 Q_o (\sigma_o^2)^{1/2} = 4\pi G r_c^2 Q_o^{2/3} \rho_o^{1/3} \quad (4)$$

Integrations can be carried out with  $\beta = 0$ , but for the above range of  $\gamma$ , the dispersion is found to increase outwards around the point of gradient change in  $Q(r)$ . As CDM simulations indicate a small radial anisotropy in the *outer* parts of a halo, at each step in the integration, trial values of  $\beta$  are stepped through (in units of 0.001) in order to determine that value which makes the logarithmic gradient in dispersion have the shallowest *negative* value. In this way a  $\beta$  profile is obtained starting at zero in the center (actually 0.001 for computational reasons) remaining small throughout the core and usually ending up  $\sim 0.2$ – $0.3$ . At some point further out the scheme tries to make  $\beta$  decrease but it is constrained to remain at its maximum value. The above value of  $\beta_{max}$  is a rough average of the outermost values determined for CDM halos (Fig. 3 of Dehnen & McLaughlin (2005)). Unlike models computed without

the above simple, well defined prescription, those here exhibit consistent scaling relations (see discussion below). Furthermore, the initial rise of  $\beta$  is very nearly a linear function of the logarithmic density gradient as advocated by Hansen & Moore (2006). Beyond  $\beta \sim 0.3$  however, both the Hansen & Moore and the Dehnen & McLaughlin results show a large scatter in  $\beta$  and we have elected to keep it constant in this region.

The core can be considered isothermal (i.e. constant velocity dispersion and negligible velocity anisotropy) within the region where the logarithmic density gradient is greater than -0.1. This radius is  $\sim 0.2 r_c$ .

Depending on what observations are given (i.e. initial rotation curve slope, the location of the bend in the rotation curve or its amplitude) determines which of the parameters  $\rho_o$ ,  $r_c$  or  $Q_o$  one chooses to fix initially. A model is constructed by integrating equations (2) and (3) while systematically varying the other two parameters until the logarithmic density gradient becomes -4.000 at  $M_{vir}^1$ .  $M_{vir}$  and  $R_{vir}$  are defined as the values of mass and radius where the mean density becomes  $100 \times \rho_c$  ( $h_{100} = 0.7$  assumed throughout). This outer boundary condition was determined empirically (e.g. by fitting the outer profile to the observations of the cluster A1689 as described below). The density profile derived from equation (2) is quite different from an NFW profile. It possesses a constant density core followed by a relatively steep radial fall-off. A steep fall-off in density appears to be demanded by the observations of galaxy cluster A1689 (Broadhurst et al. 2005) and is shown in Fig. 1. The value of  $\rho_o$  determined for a converged model corresponds to a particular value of  $\beta_{max}$ . Remarkably, any other model with *the same*  $\rho_o$  can then be obtained from the following scaling relations (i.e.  $Q_o \propto M^{-1}$ ,  $Q_o \propto \sigma_o^{-3}$  and  $Q_o \propto r_c^{-3}$ ) and hence is a member of a *one parameter* family of models. Interestingly, these scaling relations are identical to those discussed by Dalcanton & Hogan (2001) to describe the results of ‘gentle’ merging given that during a merger  $Q$  cannot increase. Based on this discussion, the inverse relation between  $Q_o$  and  $M$  found here suggests that equation (1), for all of its simplicity, is consistent with *a form of* hierarchical structure formation. As discussed by the above authors, it is decidedly not compatible with ‘phase packing’ where one expects more massive objects (with higher central velocity dispersions) to have smaller core radii.

In what follows, models are specified by the four parameters  $Q_o$  ( $M_\odot pc^{-3}(km \ sec^{-1})^{-3}$ ),  $r_c$  (kpc),  $\rho_o$  ( $M_\odot pc^{-3}$ ) and  $\alpha$  and are enclosed in brackets.

It is useful to express the equivalent *gas* entropy in terms of  $Q$ . We do this by evaluating the adiabatic constant  $K = kTn_e^{-2/3}$ . With  $Q$  in the same units as above we obtain

---

<sup>1</sup> Approximate solutions which obviate the need for the trial and error procedure are given in the appendix.

$$K = \frac{8.84 \times 10^{-7} \mu \mu_e^{2/3} ((3 - 2\beta(r))/3)}{Q^{2/3}} = K_o (3 - 2\beta(r))/3 (1 + (r/r_c)^\alpha)^{1.28/\alpha} \quad (5)$$

and  $K_o = 8.84 \times 10^{-7} \mu \mu_e^{2/3} Q_o^{-2/3} \text{ kev cm}^{-2}$

Note that the entropy of the gas is initially constant at  $K_o$  and then increases as a power law with index 1.28 as long as  $\beta$  remains constant in the outer region (see Fig. 1). We emphasize that inherent in equation (5) is the assumption that the entropy of the gas is the same as the entropy of the dark matter and that as merging continues the increase in entropy is the same for both components. Thus this value of  $K$  must be a lower limit to the actual gas entropy and as such it provides a floor on which gas physics processes (i.e. cooling, heating, astration etc.) can be played out.

The characteristics of a representative model (in this case for the galaxy cluster A1689) are shown in Fig. 1.

### 3. Confronting the Model with Observations

As a test of the model we apply it to three regimes of total mass: LSB galaxies, clusters of galaxies and dwarf spheroidal galaxies.

#### 3.1. LSB Galaxies

Hayashi et al. (2004) have derived best fit rotation curves for a sample of LSB galaxies using the NFW density profile. They divided their fits into three categories. The first (A class) provided good fits to the observations. The second (B class) included galaxies which could not be satisfactorily fit with  $\Lambda$ CDM-compatible parameters. Galaxies in the third group (C class) have irregular rotation curves. Fig. 2 shows the fits of the circular velocity  $(GM_r/r)^{1/2}$  of our model to four of the galaxies investigated by Hayashi et al. The observational data is from McGaugh et al. 2001 and is available at <http://www.astro.umd.edu/~ssm/data>. Following Hayashi et al. we let the smallest uncertainty in velocity be  $\pm 5 \text{ kmsec}^{-1}$ . The above model provides adequate fits to both class A *and* class B samples. Parameters for the class A galaxies  $(3.41 \times 10^{-7}, 1.1, 0.254, 1.92)$  for ESO2060140 and  $(1.2 \times 10^{-7}, 1.83, 0.110, 1.92)$  for F563-1 show significantly higher central densities (and  $\beta_{max}$ 's  $\sim 0.3$ ) than the B group galaxies  $(3.5 \times 10^{-8}, 5.1, 5.71 \times 10^{-3}, 1.92)$  for ESO0840411 and  $(1.68 \times 10^{-8}, 6.0, 8.28 \times 10^{-3}, 1.92)$  for UGC5750 with  $\beta_{max}$ 's 0.205 and 0.220 respectively. Generally, models with higher values of  $\rho_o$  have cores with relatively larger values of  $Q_o$ .

### 3.2. Clusters of Galaxies

The derived behavior of the dark matter density profile in the inner parts of galaxy clusters is controversial in part because of ‘contamination’ by the baryonic component in addition to the observational resolution difficulties. Here we fit our model to a recent gravitational lensing study of the massive cluster A1689 by Broadhurst et al. (2005). Standard integration of the density profile provides the run of projected mass with radius. Figure 1 shows a model with parameters  $(2.08 \times 10^{-11}, 33.4, 0.10, 1.92)$  fit to the Broadhurst et al. data. The model has a virial mass of  $1.3 \times 10^{15} M_{\odot}$ . Comparing this figure to Fig. 3 of the Broadhurst et al. paper shows that unlike the best fit NFW profile this model exhibits the desired properties of more flattening towards the center *and* more steepening towards the outside. The reduced  $\chi^2$  statistic for this particular model fit is  $\chi^2_{red} = 23.8/dof = 23.8/12 = 1.98$ .

Figure 1 shows the run of gas entropy as it would be before any astrophysical processing. Note that both the general shape and the normalization are similar to the observations of Donahue et al. (2006).

### 3.3. The Fornax Dwarf Spheroidal Galaxy

Recently Goerdt et al. (2006) and Sánchez-Salcedo et al. (2006) have argued that the Fornax dwarf must contain a large core in order that its globular clusters are not drawn into the center by dynamical friction. In order to test the sensitivity of this process to core size, two models were constructed. One has parameters  $(1.36 \times 10^{-5}, 0.385, 0.1, 1.92)$  and  $\beta_{max} = 0.294$  while the other has  $(3.46 \times 10^{-6}, 0.920, 1.31 \times 10^{-2}, 1.92)$  and  $\beta_{max} = 0.237$ . Both have the same virial mass of  $1.99 \times 10^9 M_{\odot}$ . (Note that the value of  $r_c$  of 0.92 kpc provides a region within which the logarithmic density gradient is less than -0.1 of only  $\sim 0.2$  kpc consistent with Goerdt et al.) The dynamical friction time scales can be compared using the following expression from Henon (1973) (i.e.  $\tau_{df} \approx 4 \times 10^9 V^3 / (\ln(\Lambda) M_{GC} \rho)$  yrs). Here,  $V$  is the velocity of the cluster with assumed mass  $M_{GC} = 2 \times 10^5 M_{\odot}$  and  $\ln \Lambda$  is the coulomb logarithm which we take here to be 5 for consistency with Goerdt et al. Given that within the radial distance  $\sim 0.2 r_c$  the density and velocity dispersion are essentially constant and  $\beta \sim 0$ , we replace  $V^3/\rho$  with  $3\sqrt{3}\sigma_o^3/\rho_o = 3\sqrt{3}/Q_o$  and obtain

$$\tau_{df} \approx \frac{5.2 \times 10^9}{M_{GC} Q_o} \text{ yrs} \quad (6)$$

While the above estimate for  $\tau_{df}$  is no substitute for a Goerdt et al. type of analysis, it does allow an intercomparison among our cored models.

The above model with the largest core has a dynamical friction time scale of  $7.5 \times 10^9$  years which is nearly four times that of the cluster with the smaller but higher density core.

As a further check, a model with the same mass and  $r_c$  but different  $\alpha$  was made with parameters  $(4.25 \times 10^{-6}, 0.920, 1.49 \times 10^{-2}, 1.0)$ . The region within which the density gradient is less than -0.1 now has a radius of only 0.05 kpc. As expected, its dynamical friction time scale is shorter than the above model with the same  $r_c$  but only by  $\sim 18\%$ . (Lowering  $\alpha$  while keeping the other parameters the same lowers the central entropy slightly). This simple analysis is in accord with the conclusions of Goerdt et al. and Sánchez-Salcedo et al. that increasing the core size leads to an increase in dynamical friction time scale. This increased time scale approaches a Hubble time and because our calculated value of  $Q_o$  is *not* necessarily assumed to be a result of phase packing remains within the constraints imposed by the sophisticated dynamical model of Fornax by Strigari et al. (2006).

An additional check on the model comes from the recent work of Gilmore et al. (2007) whose analysis of the light distribution and velocity dispersion profile of several local dwarf spheroidal galaxies shows that shallow (cored) central density profiles with mean densities of  $0.1 M_\odot pc^{-3}$  (identical to that of our model above with  $r_c = 0.385 kpc$ ) are most consistent with the observations.

## 4. Discussion

A new model for dark matter halos has been proposed and is successfully applied to observations of objects with masses ranging from  $\sim 10^9$  to  $\sim 10^{15} M_\odot$ . Fig. 3 is a graphical summary of the results which shows the scaling relations discussed earlier. It is important to note key differences in structure occur with different scaling normalizations. The filled symbols are structures with relatively high values of  $\rho_o$  ( $\sim 0.1 M_\odot pc^{-3}$ ) while the open symbols are structures with lower values of  $\rho_o$  ( $\sim 0.01 M_\odot pc^{-3}$ ) and lower  $\beta_{max}$ 's. Close examination of Fig. 3 reveals a real systematic shift between these two groups of objects. Objects with identical central densities would lie essentially dispersionless along a line of the indicated slope. Further, for two models with the same mass, the one with the higher  $Q_o$  has the higher  $\rho_o$  and smaller  $r_c$  (i.e. quantitatively  $\partial \log Q_o / \partial \log \rho_o = 0.67$  and  $\partial \log Q_o / \partial \log r_c = -1.57$  for a fixed halo mass). While the density is not expected to increase during merging, Hernquist et al. (1993) propose a scheme whereby the density decreases while the dispersion remains constant. Dalcanton & Hogan interpret this as a result of more violent merging so that different merging histories at earlier times could account for the variations in central density seen now. More observations are required to determine if the apparent dichotomy in central density is real and if so what its origin is. For example, if we assume

that the dichotomy extends to galaxy clusters, then a model with the same mass as A1689 but with one tenth the central density will have its gas entropy floor raised by  $\sim 2.8$ . Such a change in central gas entropy floor is one characterization differentiating cooling flow clusters from non cooling flow clusters.

The error bars in each panel of Fig. 3 were calculated by assuming an empirical approximation to  $\gamma$  (equation (4)) in terms of the central density (i.e.  $\gamma \sim 1.80\rho_o^{-0.0753}$ ) and variables  $\rho_o$  and  $r_c$  were then treated as independent with estimated uncertainties of  $\pm 0.25$  and  $\pm 0.10$  respectively.

Rotation curves derived from the model and the NFW profile can be very similar (e.g. the two A class galaxies in §3.1) while according to the model the data appear incompatible with standard CDM cosmological simulations which do not predict ‘observable-sized’ cores. The similarity is most pronounced among objects in the high central density group. One property of our cored models which may be relevant to the ‘missing satellite’ problem is that these structures are more vulnerable to tidal disruption than the NFW models, especially those halos with low central densities.

From this work a relation has been determined between  $Q_o$  and the mass of dark matter halos over a range from  $\sim 10^9$  to  $\sim 10^{15} M_\odot$ . An observational challenge is to find the lower mass limit to objects with dark matter halos thus providing an estimate of the primordial value of  $Q$  ( $Q_p$ ). Knowledge of  $Q_p$  allows the determination of the mass of the dark matter particle (assuming that the particles are thermal) since then  $Q$  is proportional to the fourth power of the particle mass (e.g. equating the value of  $Q_o$  found above for Fornax with  $Q_p$  provides a lower limit on this mass of 431 eV). An additional constraint comes from an analysis of the power spectrum of the Ly $\alpha$  forest. From this one can determine the free streaming length ( $\lambda_{fs}$ ) of the dark matter particle. This quantity in turn is simply related (in the case of thermal particles) to the particle mass. A recent determination of a limit on  $\lambda_{fs}$  by Seljak et al. (2006) implies a thermal dark matter particle mass limit of  $> 10$  keV (i.e.  $Q_p > 1$  which according to our scaling relation above implies dark matter halos with masses as low as  $\sim 10^3 M_\odot$ ).

An attractive alternative to the above ‘classical’ WDM scenario has been proposed by Strigari et al. (2007). If the particles are non-thermally produced by the decay of a supersymmetric particle for example and if they are born sufficiently late then the initial velocities of the resulting daughter particles can be sufficiently high to yield a free streaming length comparable to that found from the Ly $\alpha$  forest analysis but with  $Q_p$  orders of magnitude lower than above (i.e.  $Q_p \sim 10^{-5} - 10^{-6}$ ) and a correspondingly much higher dark halo mass limit. This picture has the additional feature that it is hierarchical in the conventional CDM sense since the parent particles are born cold and being bosons they are not subject to the



ultimate phase space density restriction.

Future results from experimental particle physics and even more sophisticated cosmological simulations should lead to a fuller understanding of the dark matter problem and the viability of the model.

The author wishes to thank Drs. Julio Navarro, Tony Burke and Andi Mahdavi for useful discussions, Dr. Greg Poole for introducing me to x-ray observations of galaxy clusters and the referee for a constructive report.

## REFERENCES

- Binney, J., & Tremaine, S. 1987, *Galactic Dynamics*, (Princeton: Princeton University Press)
- Broadhurst, T., Takada, M., Umetsu, K., Kong, X., Arimoto, N., Chiba, M., & Futamase, T. 2005, *ApJ*, 619, L143
- Burkert, A. 1995, *ApJ*, 447, L25
- Dalcanton, J.J., & Hogan, C.J. 2001, *ApJ*, 561, 35
- Dehnen, W., & McLaughlin, D.E. 2005, *MNRAS*, 363, 1057
- Dekel, A. & Arad, I. 2004, in “Satellites and Streams”, eds F. Prada, D. Martinez-Delgado & T.J. Mahoney (San Francisco: ASP) p. 303
- Donahue, Megan, Horner, Donald J., Cavagnolo, Kenneth W., Voit, G. Mark 2006, *ApJ*, 643, 730
- Gilmore, G., Wilkinson, M.I., Wyse, R.F.G., Kleyna, J.T., Koch, A., Wyn Evans, N., & Grebel, E.K. 2007, *astro-ph/0703308*
- Goerdt, Tobias, Moore, Ben, Read, J. I., Stadel, Joachim, Zemp, Marcel 2006, *MNRAS*, 368, 1073
- Graham, A. W., Merritt, D., Moore, B., Diemand, J., & Terzic, B. 2006, *AJ*, 132, 2701
- Hansen, S. H., & Moore, B. 2006, *New Astronomy*, 11, 333
- Hayashi, E., Navarro, J. F., Power, C., Jenkins, A., Frenk, C. S., White, S. D. M., Springel, V., Stadel, J., & Quinn, T. R. 2004, *MNRAS*, 355, 794
- Henon, M., 1973, *Dynamical Structure and Evolution of Stellar Systems*, Third Advanced Course of the Swiss Society for Astronomy and Astrophysics, p. 183. (Geneva Observatory)

- Hernquist, Lars, Spergel, David N., & Heyl, Jeremy S. 1993, ApJ, 416, 415
- Kochanek, C.S. & White, M. 2000, ApJ, 543, 514.
- McGaugh, Stacy S., Rubin, Vera C., & de Blok, W. J. G. 2001, AJ, 122, 2381
- Merritt, D., Graham, A. W., Moore, B., Diemand, J., & Terzic, B. 2006, AJ, 132, 2685
- Navarro, Julio F., Frenk, Carlos S., & White, Simon D. M. 1997, ApJ, 490, 493
- Sánchez-Salcedo, F. J., Reyes-Iturbide, Jorge, & Hernandez, X. 2006, MNRAS, 370, 1829
- Sand, David J., Treu, Tommaso, & Ellis, Richard S. 2002, ApJ, 574, L129
- Seljak, Uros, Makarov, Alexey, McDonald, Patrick, & Trac, Hy 2006, Phys. Rev. Lett., 97, 191303
- Strigari, Louis E., Bullock, James S., Kaplinghat, Manoj, Kravtsov, Andrey V., Gnedin, Oleg Y., Abazajian, Kevork, & Klypin, Anatoly A. 2006, ApJ, 652, 306
- Strigari, Louis E., Kaplinghat, Manoj, & Bullock, James S. 2007, Phys. Rev. D, 75, 061303
- Taylor, James E., & Navarro, Julio F. 2001, ApJ, 563, 483
- Tremaine, S., & Gunn, J.E. 1979, Phys. Rev. Lett., 42, 407

## Appendix

As described above, a converged model is obtained by the somewhat cumbersome trial and error method. Below we present some analytical approximations which will allow a more efficient exploration of parameter space and which illustrate more explicitly the two (scaling) parameter nature of the model (i.e. fix  $\rho_o$  and vary  $Q_o$ ). They were obtained by ‘fitting’ to the converged solutions above. Letting  $\alpha = 1.92$  in equation (1) of the text, the density profile is approximated by

$$\rho(r) \sim \frac{\rho_o}{(1 + (r/r_c)^{1.92})(1 + (r/(\delta(\rho_o)r_c))^{2.08})} \quad (1)$$

where

$$r_c \sim 5.773 \times 10^{-3} \rho_o^{-0.2043} Q_o^{-1/3} \quad (2)$$

and

$$\delta(\rho_o) \sim 6.93 \log \rho_o + 24.97 \quad (3)$$

The velocity dispersion becomes

$$\sigma^2(r) \sim \frac{(\rho_o/Q_o)^{2/3}}{(1 + (r/(\delta(\rho_o)r_c))^{2.08})^{2/3}} \quad (4)$$

Finally the value of  $\beta_{max}$  is obtained by determining the maximum associated with the smallest  $r$  value (i.e. the first maximum) in the following expression

$$\beta(r) \sim -0.5GM_r/(\sigma^2r) - 0.5 d \log Q/d \log r - (5/6)d \log \sigma^3/d \log r \quad (5)$$

where  $M_r$  comes from the integration of equation (3) in the text.

With these approximations, values of  $r_c$ ,  $M_{100}$ ,  $R_{100}$ , are determined to  $< 1\%$ ,  $< 4\%$ , and  $< 2\%$ . Deviations in  $\beta_{max}$  are between 1.4% and 14.1% with the largest deviations occurring at the lowest values of  $\rho_o$ . Beyond the maxima the run of  $\beta$  is not reliable. Circular velocity maxima derived from the above expressions are within 5% of the model values. It should be emphasized that the above expressions and bounds were determined from models with central densities  $5.7 \times 10^{-3} \leq \rho_o \leq 2.54 \times 10^{-1}$ .

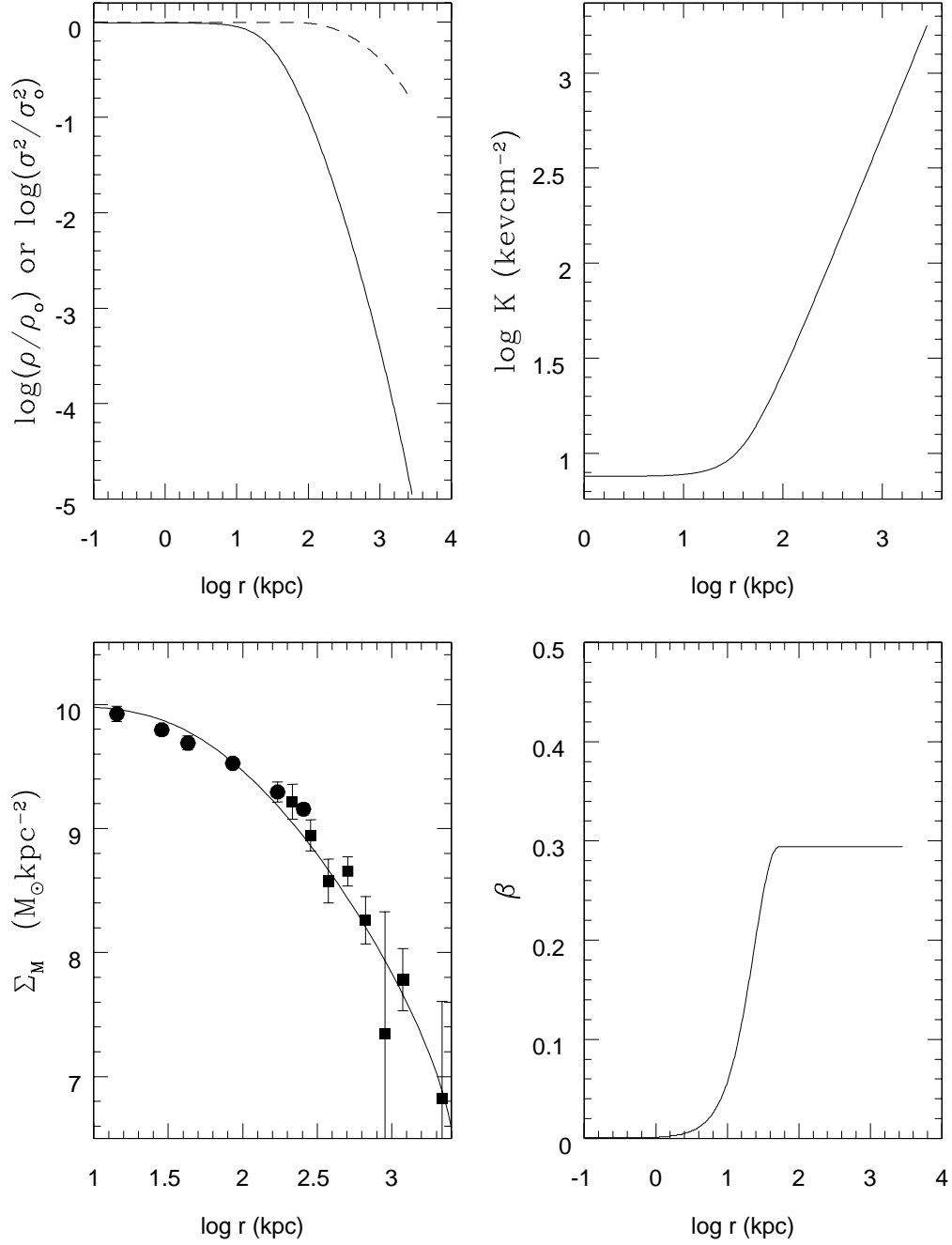


Fig. 1.— Attributes of a solution to equations (1),(2),& (3) for the galaxy cluster A1689. Upper left panel: The run of density (solid) and velocity dispersion (dashed) versus radial distance. Upper right panel: The gas entropy profile before astrophysical processes change it. Lower left panel: Observational data from Fig. 3 of Broadhurst et al. 2005 with the model projected mass density superposed. Lower right panel: The run of  $\beta$  with radial distance derived as described in §2.  $\log(r_c)$  for this model is 1.52.

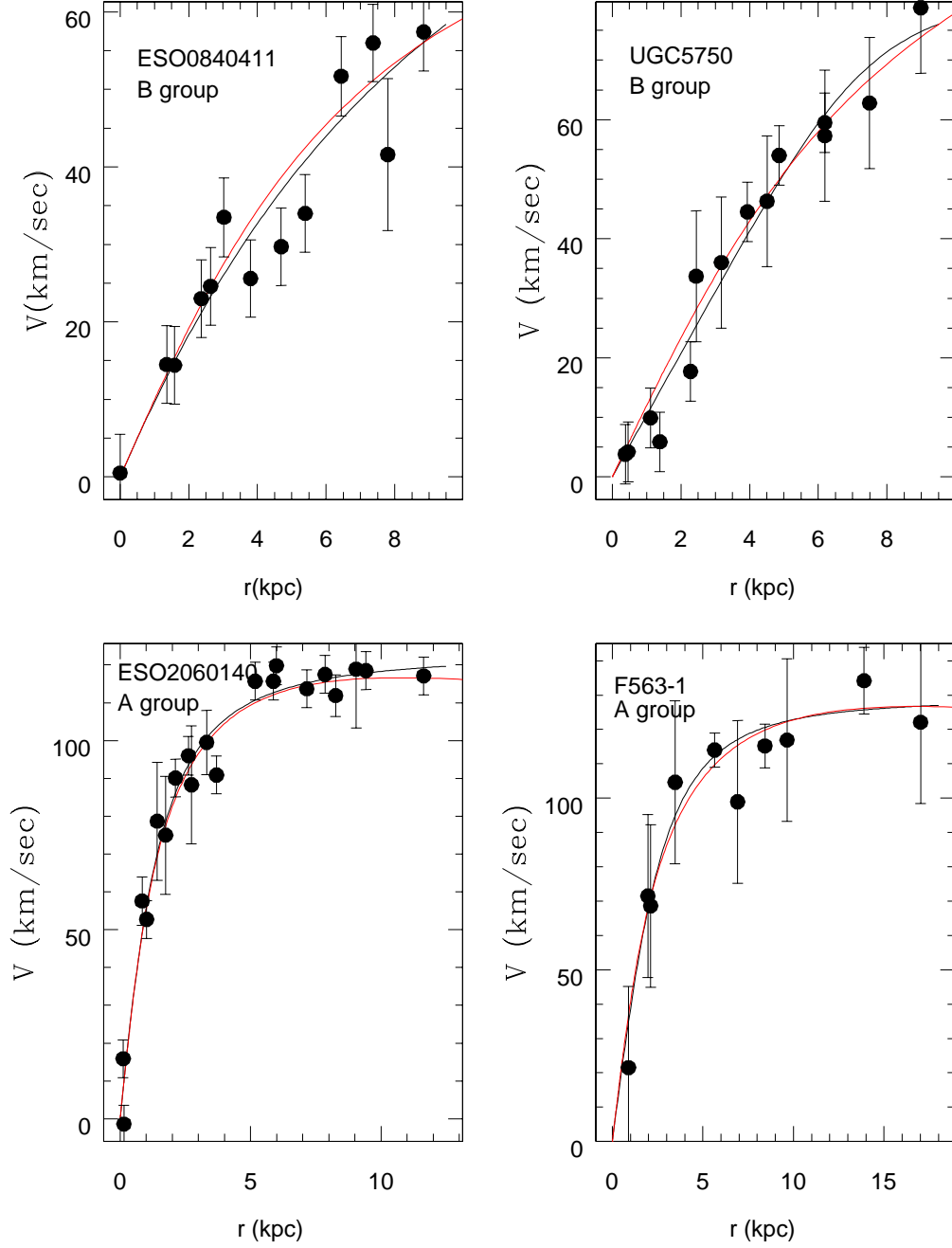


Fig. 2.— Model fits to LSB galaxy rotation curves. The black line is the fit of an empirical fitting function with the same parameters given in Figs 7 & 8 of Hayashi et al. 2004. The red curve is the model fit. Recall that NFW profiles could not be well fit to the two group B galaxies. The reduced  $\chi^2$  for all model fits is  $< 1$ .

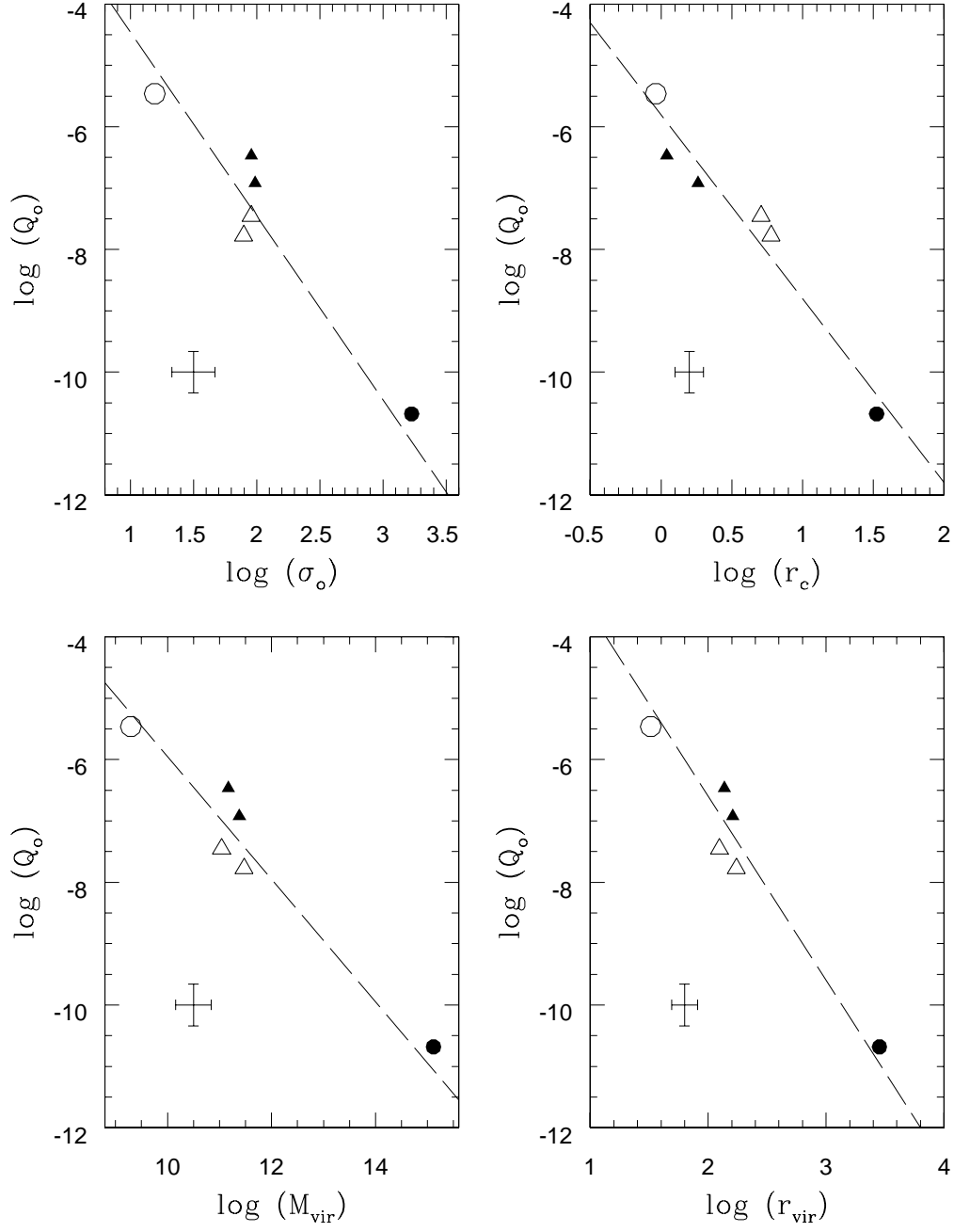


Fig. 3.— The model parameters for the six systems discussed here. Open circle- Fornax dwarf, open triangles-group B LSB galaxies, solid triangles-group A LSB galaxies and solid circle-galaxy cluster A1689. Clockwise from the upper left shows  $\log(Q_o)$  versus central velocity dispersion, core radius, virial radius and virial mass. The dashed lines are not fits but illustrate the scaling relations described in the text (i.e.  $Q_o \propto \sigma_o^{-3}$ ,  $\propto r_c^{-3}$ ,  $\propto r_{vir}^{-3}$  and  $\propto M_{vir}^{-1}$ ).